Theor Chem Acc (2011) 128:705–711
DOI 10.1007/s00214-010-0854-z

REGULAR ARTICLE

On the photoproduction of DNA/RNA cyclobutane pyrimidine dimers

Israel González-Ramírez · Daniel Roca-Sanjuán · Teresa Climent · Juan José Serrano-Pérez · Manuela Merchán · Luis Serrano-Andrés

Received: 31 August 2010 / Accepted: 3 November 2010 / Published online: 23 November 2010

Abstract The UV photoreactivity of different pyrimidine DNA/RNA nucleobases along the singlet manifold leading to the formation of cyclobutane pyrimidine dimers has been studied by using the CASPT2 level of theory. The initially irradiated singlet state promotes the formation of excimers between pairs of properly oriented nucleobases through the overlap between the π structures of two stacked nucleobases. The system evolves then to the formation of cyclobutane pyrimidine dimers via a shearing-type conical intersection activating a [2 + 2] photocycloaddition mechanism. The relative location of stable excimer conformations or alternative decay channels with respect to the reactive degeneracy region explains the differences in the photoproduction efficiency observed in the experiments for different nucleobases sequences. A comparative analysis of the main structural parameters and energetic profiles in the singlet manifold is carried out for thymine, uracil, cytosine, and 5-methylcytosine homodimers. Thymine and uracil dimers display the most favorable paths, in contrast to cytosine. Methylation of the nucleobases seems to increase the probability for dimerization.

Keywords CASPT2 · Photochemisty · Conical Intersection · DNA/RNA · Cyclobutane Pyrimidine Dimers

Published as part of the special issue celebrating theoretical and computational chemistry in Spain.

I. González-Ramírez · T. Climent · M. Merchán · L. Serrano-Andrés
Instituto de Ciencia Molecular, Universitat de València, P. B. Box 22085, 46071 Valencia, Spain

D. Roca-Sanjuán (✉)
Department of Quantum Chemistry, Uppsala University, Box 518, 75120 Uppsala, Sweden
e-mail: Daniel.Roca@kvac.uu.se

J. J. Serrano-Pérez
Department of Chemistry, Computational and Structural Research Group, Imperial College London, SW7 2AZ London, UK

1 Introduction

The UV radiation directly absorbed by the nucleic acids can produce a large number of lesions [1, 2], the most common corresponding to dimer or adduct formations involving adjacent pyrimidine bases of the DNA/RNA strand [3–7]. Two types of dimerized products are frequently found: the cyclobutane pyrimidine dimers (CPDs), in which the adduct is formed via a [2 + 2] photocycloaddition involving the C=C double bonds of the pyrimidines, and the pyrimidine (6-4) pirimidone dimers, usually referred to as (6-4) photoproducts, (6-4)PPs, in which the cycloaddition takes place between C=C and C=O double bonds of the adjacent molecules. CPD lesions are more frequent than (6-4)PPs [3, 4]. Under UV-C (254-nm) radiation conditions, between two and ten CPDs per million bases are formed [5]. Two more orders of magnitude of lower-energy UV-B radiation are required to obtain the same result. Even though, in theory, various CPD diastereoisomers are possible, only the *cis-syn* conformer is found in the double helix. The *trans-syn* configuration can be also obtained, with lower yields, in single or double strands of denaturalized DNA, where the tertiary and secondary structure are lost to some extent with respect to the standard double helix [3]. Although the pyrimidine bases can react to form CPDs in many combinations, we will focus here on the homodimers of the canonical DNA/RNA bases thymine (T), uracil (U), cytosine (C) (and their adducts

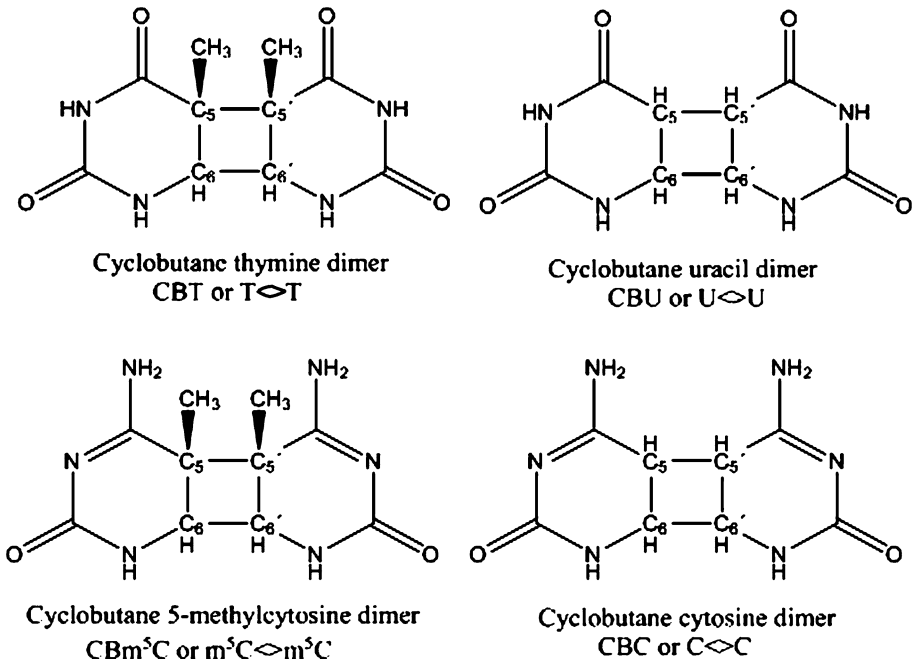

Fig. 1 Structures and labeling of the DNA/RNA cyclobutane pyrimidine homodimer photoproducts

CBT, CBU, and CBC), and on the derivative 5-methylcytosine (m^5C and CBm^5C), as displayed in Fig. 1.

Despite all CPDs can be considered DNA/RNA lesions, not all of them are actually mutagenic hotspots, something that depends on the rate of the enzymatic repair mechanisms or of the transitions from one pyrimidine to another, for instance by deamination plus ketonization in C and m^5C to U and T, respectively. Therefore, despite CBT dimers are more frequently found among the photodimers detected in DNA in different conditions [6], CC and m^5Cm^5C sites are potentially more damaging, because they might efficiently give rise to an actual mutation. Additionally, and in general, CPDs seem to undergo more rapid deamination than individual nucleobases [8–11]. The important role of the noncanonical m^5C derivative [12], which is found in significant amounts in the DNA of many eukaryotic organisms (5% in human and calf thymus DNA and 31% in wheat DNA [13, 14]), is recognized since a decade ago. Whereas earlier works were unsuccessful in detecting significant amounts of m^5C-containing CPDs [15, 16], it was found later that cyclobutane dimers of m^5C are formed when irradiated with either UV-C or UV-B [12, 17, 18] and that methylation increases the photoproduction with respect to the canonical nucleobase [17]. Tommasi et al. [18] analyzed the CPDs formation in different combinations of pyrimidine nucleobases irradiated with UV-C, UV-B, and sunlight. The methylated DNA base m^5C was the preferred target for CPD production when the natural sunlight was used.

Femtosecond spectroscopy has proved that T-dimerization is an ultrafast photoreaction in which CBTs are fully formed $\sim$1 ps after UV illumination [19]. From a theoretical standpoint, a few studies have confirmed for CBC [20] and CBT [21–24] dimers an ultrafast nonadiabatic photoreaction involving a barrierless path along the low-lying singlet excited (S_1) state. The concerted mechanism for the [2 + 2] photocycloaddition of two C- or T-molecules is mediated by the presence of a conical intersection (CI), an energy-degenerate structure between the low-lying singlet excited (S_1) and the ground state (S_0). The shearing-type CI structure—in which the nucleobases ethylenic C_5–C_6 and C_5'–C_6' bonds laid parallel (parallelogram type) and elongated—, connects the S_1 and S_0 states and allows an efficient internal conversion process [20]. Intrastrand nucleobase sequence and relative orientations were also proved to be essential for an efficient photoreaction to take place. In previous works on CC, TT, and UU pairs [20, 23, 25], we showed that those conformations maximizing the overlap between the π structures of stacked nucleobases formed favorable excimer arrangements, being the most stable structures leading to the photoreactive arrangements, in agreement with the higher yields obtained for photoproducts with *cis*-type parallel face-to-face conformations for the base pairs. Additionally, we determined that the formation of CPDs can be also obtained in the triplet manifold through a biradical intermediate involving a singlet–triplet crossing $(S_0/T_1)_X$ relating the ground (S_0) and low-lying triplet state (T_1) [20, 26, 27], and explaining the high yields of CPDs detected in solution in presence of external photogenotoxic substances acting as triplet–triplet photosensitizers [3, 28, 29].

Obtaining an accurate mapping of the relative energies of the excimer and CI structures in the different dimers is crucial to understand the formation mechanisms and the observed photoreaction yields. Earlier, we attributed the low yield measured for the CBC formation when compared to CBT to the competitive presence of stable excimer conformations and the CI responsible for nucleobase monomer deactivation (CI_{mon}) at energies similar or lower than the [2 + 2] photocycloaddition sheared-type CI (CI_{dim}) in CC. In contrast, for TT CI_{dim} is the most stable structure [23, 26], favoring the reactive process. The goal of the present contribution is to complement the theoretical study on the CPDs formation in cytosine and thymine homodimers with the analysis of the photodimerization in the other pyrimidine nucleobase, uracil, and the noncanonical C_5-methylated cytosine base, providing a wider overview of the photodimerization process in pyrimidines. It is intended to give a rationale on the predominant presence of some specific photodimers over others in terms of the differences found among the potential energy hypersurfaces of the ground state and the lowest excited state related to the [2 + 2] photocycloaddition. Concerning U and m^5C, and except for a previous DFT study on m^5C [30], to our knowledge no reliable study at the required multiconfigurational level has been reported. Therefore, the present work is the first ab initio theoretical determination of the mechanism of photodimerization in uracil and the noncanonical m^5C nucleobase, allowing an overall comparison of the CPDs formation mechanisms for the most important nucleobases homodimers.

2 Methods and computational details

In order to provide a comparative study of the cyclobutane dimer formation in pyrimidines, the same methodology as that previously employed in the cytosine and thymine homodimers has been used in the present work for the theoretical determination of the mechanism of photodimerization of two uracil and two 5-methylcytosine dimers [20, 23, 26]. The ANO-S basis set contracted to C,N,O[3s2p1d]/H[2s1p] was used throughout. Multiconfigurational CASPT2(14/10) and CASPT2(12/12) calculations [31–34] were performed, respectively, for the monomers and the dimers. This included CASSCF geometry optimizations of the singlet states minima, minimum energy paths (MEPs), and minimum energy crossing points (MECPs) determinations in the potential energy hypersurfaces (PEHs) of a system of two nucleobases, corrected at the CASPT2 level using point-wise calculations [20, 35]. Energies were also corrected on the effect of the basis set superposition error (BSSE) using the counterpoise (CP) procedure [20, 36]. As shown previously [20, 25, 37], the inclusion of BSSE is crucial to accurately describe the binding energies and compare the different mechanisms. The MOLCAS quantum-chemistry code was employed throughout [38]. In order to minimize weakly interacting intruder states, the imaginary level-shift technique with a parameter 0.2 au has been employed [39]. In order to mimic the interaction of pyrimidines in the biologically relevant *cis-syn* diastereoisomer, geometry optimizations were initially performed within the constraints of the C_s symmetry. Since the CASSCF structures of the dimer on the MECPs do not represent a crossing at the CASPT2 level, MECPs were finally obtained with the CASPT2 methodology. Further technical details can be found in previous publications [20, 23].

3 Results and discussion

As mentioned in the introduction, previous experimental and theoretical studies [19–23, 40, 41] determined a general mechanism for the ultrafast photoproduction of CPDs in nucleobases oligomers strands. It is suggested that after initial radiative population of delocalized exciton states on the nucleobases multimers, the system evolves in an ultrafast manner to either a localized excited state of the nucleobase monomer or a fluorescent excimer/exciplex state, depending on the smaller or larger degree of stacking, respectively [37]. Relaxation along the monomer path should be ultrafast ($\tau < 2$ ps), as known in the isolated systems [34, 42, 43], whereas from the long-lived excimer/exciplex state the system is expected to decay to the ground state slowly ($\tau > 10$ ps). The slower relaxation paths for the stacked nucleobases, expanding from 10 to 200 ps, have been found dominant in the decay dynamics of dinucleotides after excitation at 267 nm (4.96 eV) [19], and it can be assigned to the formation of more or less stable excimer/exciplex structures. There are additional accessible evolution paths for the pairs of bases, in particular for pyrimidine nucleobases, in which the excimer/exciplex behave as precursor for the formation of cycloadducts like CPDs or (6-4)PPs dimerized structures. As shown, there is always a $(S_0/S_1)_{CI}$ degeneracy region responsible for the photoprocess to take place. In order to elucidate the basics of the relaxation mechanisms in DNA photochemistry, it is required to provide a common framework in which all basic structures—CI of the monomer, excimers, and CI of the photoreaction—are determined at the same level of theory. The comparison between the mechanisms of photodimerization in the considered nucleobases will help to explain the distinct efficiency for photodimers production found in the experiments. Table 1 contains the relative energies, with respect to two isolated nucleobases in the ground state and selected

Table 1 Selected structural distances (R/Å) and energies (ΔE/eV) of the relevant structures along the singlet manifold in the photoproduction mechanism of cyclobutane pyrimidine dimers

Monomer/homodimer	R (C_5–C_5')	R (C_6–C_6')	ΔE
Mon (S_1)			
C* + C	–	–	4.41[a]
m^5C^* + m^5C	–	–	4.31[b]
U* + U	–	–	5.02[a]
T* + T	–	–	4.89[a]
CI_{mon} $(S_1/S_0)_{CI}$			
C	–	–	3.60[a]
m^5C	–	–	3.64[b]
U	–	–	3.90[a]
T	–	–	4.00[a]
Exc (S_1)			
C*C	3.427	3.219	3.31[c]
$m^5C^*m^5C$	3.594	3.346	3.46
U*U	2.503	2.315	3.68
T*T	2.650	2.380	3.64[d]
CI_{dim} $(S_1/S_0)_{CI}$			
CC	2.258	2.170	3.51[c]
m^5Cm^5C	2.491	2.056	3.56
UU	2.218	2.170	3.47
TT	2.350	2.220	3.26[d]
$(CPD)_{S0}$			
CBC	1.611	1.601	0.78[c]
CBm^5C	1.648	1.593	0.71
CBU	1.601	1.568	0.23
CBT	1.637	1.595	0.40[d]
$(CPD)_{S1}$			
CBC	1.611	1.601	5.35[c]
CBm^5C	1.648	1.593	5.63
CBU	1.601	1.568	5.87
CBT	1.637	1.595	5.88[d]

All energies are referred to the singlet ground state of two isolated nucleobases (see Figs. 2 and 3)

[a] Ref. [34]

[b] This work

[c] Ref. [20]

[d] Ref. [23]

geometry parameters for the five relevant structures in the photodimerization mechanism in the singlet manifold: the monomeric UV absorption (Mon), the monomer CI (CI_{mon}), the excimer minimum (Exc), the dimer CI (CI_{dim}), and the photodimer (CPD) in the four homodimers studied here: thymine, uracil, cytosine, and 5-methylcytosine. Figure 2 summarizes the basics of the mechanism.

UV solar radiation extends from the edge of the visible light at 400 nm (3.1 eV) to the far UV range (200 nm, 6.2 eV) and beyond. As mentioned previously, the yield of

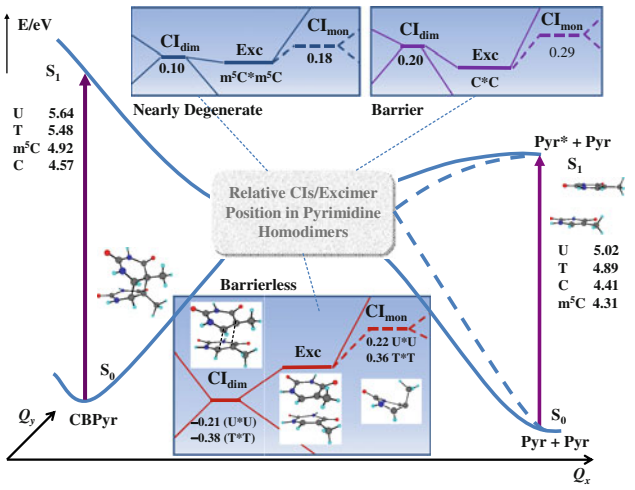

Fig. 2 Proposed scheme, based on actual CASPT2 results, for the decay path of the lowest singlet excited state S_1 of the U, T, C, and m^5C dimers involving the relaxed excimer and the conical intersection $(S_1/S_0)_{CI}$ leading to ground state cyclobutane pyrimidines (CBPyr or CPDs). Values inside the *boxes* correspond to the energies of the conical intersection of the dimer (CI_{dim}) and the monomer (CI_{mon}) structures with respect to the lowest-energy excimer (Exc). TT structures shown as an illustration

photoproduction of CPDs is wavelength dependent and increases with the energy of the absorbed radiation, because the available excess energy required to surmount energy barriers is larger for high-energy irradiations. In any case, the photoreactive process takes place ultimately in the S_1 excited state. The vertical excitation energy computed for the S_1 (HOMO → LUMO) state ranges from 4.3 eV in m^5C to 5.0 in U for the four studied nucleobases. Independently from the procedure that the S_1 is reached—directly or from decay from higher-lying singlet states—the nucleobases strand will find many arrangements in which two of the monomers will overlap their π structures, yielding very favorable conformations ready to evolve toward stable excimer/exciplex (excimer here since we are dealing with homodimers) minima in the excited state. Even when for weakly stacked pairs the excitation may localize in the monomer and decay to the ground state of the nucleobase through the CI_{mon} $(S_0/S_1)_{CI}$ (see Table 1), many arrangements will be favorable for the formation of excimers. Even in their most common biological conformation, B-DNA, it is considered that nucleobases form weakly interacting or static excimers [37]. These two types of situations, decay in the monomer through localization with access to the monomer CI and formation of excimers, can be considered responsible for the ultrafast (>2 ps) and fast (>10 ps) decays observed in femtosecond transient absorption experiments, especially in purine strands [19].

Although different excimer arrangements of distinct stability are possible, we have obtained the most stable

excimer in the four homodimers studied here as a face-to-face quasi-parallel conformation that maximizes the π overlap (see Fig. 3 as an example). At the minimum (see Table 1), the intramolecular distances between the analogous C=C double bond atoms of the adjacent monomers ($\sim$2.3–2.6 Å) are almost one Å shorter for T*T and U*U when compared to the other homodimers. T*T and U*U seem to display a stronger interaction (probably because of the two carbonyl groups), showing bonding energies with respect to the isolated monomers near 1.3 eV. In contrast, C*C and m^5C*m^5C have larger intermonomer distances ($\sim$3.2–3.6 Å) and lower binding energies ($\sim$0.9–1.1 eV). The four homodimers have also a CI degeneracy region connecting the excited S_1 and the ground S_0 state in which the system displays very similar structures, with the two monomers arranged in a quasi-parallel shearing-type conformation (see Fig. 3). This CI_{dim} $(S_0/S_1)_{CI}$ structure is responsible for the nonadiabatic [2 + 2] cyclophotoaddition reaction leading from the pair of stacked nucleobases to the final CPD photoproduct in the ground state.

The relative position of the most stable excimer conformation and the CI_{dim} $(S_0/S_1)_{CI}$ region is different in the four homodimers studied. For TT and UU pairs, CI_{dim} is the lowest-energy structure of all studied S_1 hypersurface, lying near 0.4 and 0.2 eV, respectively, below the stable excimer. It is not surprising that all the computed minimum energy paths (MEPs) in TT leads in a barrierless way from different excimer arrangements to the CI_{dim} structure [21–23], as it is the case here with UU. Additionally, the CI_{dim} structure is near 0.7 (TT) and 0.4 eV (UU) lower in energy than the CI of the respective monomers, T and U. Therefore, there is no decay process that can efficiently compete with the access to CI_{dim} and subsequent nonadiabatic

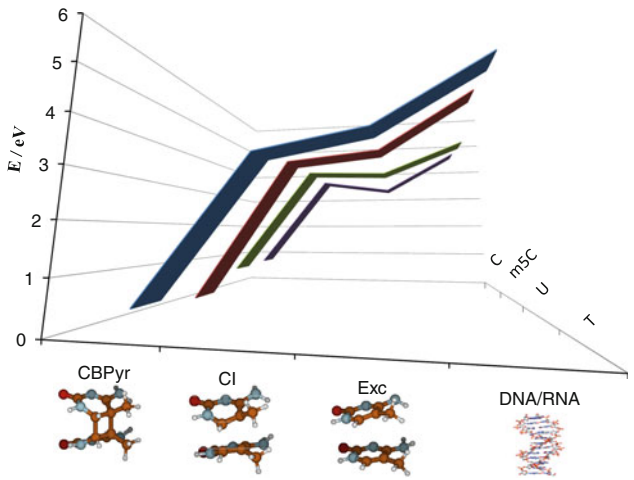

Fig. 3 Comparison of the photoreactive pathways leading to CPDs (or CBPyrs) formation along the singlet manifold for the C, m^5C, U, and T base pairs. The m^5Cm^5C structures obtained in this work are shown

transfer of energy to reach CBT or CBU, except for those systems evolving toward the splitting of the monomers. The described PEH profile is perfectly compatible with the observed high yields of production of CBT and CBU when compared with other adducts [3].

Regarding CC and m^5Cm^5C, the CI_{dim} structure has been computed 0.2 and 0.1 eV, respectively, higher in energy than their relaxed excimer minima. That means that there exist conformations that will become competitive with the nonadiabatic reaction, decreasing the rate and yield of the photoprocess in the two systems, especially in CC. The same argument can be used when comparing the dimer CI with the monomer CI, which is energetically just 0.1 eV above in both cases, opening a new decay route which may compete efficiently with the formation of CBC and CBm^5C. Overall, the lower yields observed for CC tandems in contrast to TT [44] can be therefore understood by the presence in C-based dimers of several competitive structures—stable excimers and monomer decay routes—close in energy to the reactive CI. Regarding the comparison of CC and m^5Cm^5C, the former displays excimer structures somewhat more stable with respect to the CI_{dim} (0.2 eV) than in the case of the methyl derivative, in which CI_{dim} and excimer become almost degenerate. Even when the difference is small in both cases, this profile may explain the slightly higher efficiency found in the production of m^5C dimers [12, 17]. Figure 3 depicts a scheme of the relative energy levels for the studied systems.

With respect to the geometry of the dimer CI in the four systems studied (rhomboid or parallelogram type, typical of the [2 + 2] cycloaddition [20]), and although the structural discrepancies are small, they might be relevant (see Fig. 3). Whereas the C_6–C_6' distance remains similar in the various cases, C_5–C_5' shows much more noticeable differences, reflecting a major or minor distortion with respect to the ideal rhomboid geometry. Hence, the m^5C dimer presents the most distorted structure, with the largest C_5–C_5' distance, 2.491 Å, among the studied bases. This elongation is probably a consequence of the steric effect caused by the presence of both the methyl and amino groups. Thymine, also with a methyl group, comes next with a value of 2.350 Å, followed by the less distorted cytosine and uracil systems, with distances of 2.258 and 2.218 Å, respectively. As it could be expected, methylation increases the C_5–C_5' bond length in all computed structures, excimers, CIs, and adducts.

Once the CI_{dim} crossing is reached, dimers can evolve, in an ultrafast process, to form cyclobutane pyrimidines, whose structure is shown for the m^5C in Fig. 3. The singlet pathway represented in this figure and Fig. 2 allows us to better understand the photodimer production mechanism that operates after the initial excitation taking place in DNA/RNA strands. Also, photodimers can absorb UV light

to finally obtain the separated base monomers through a photoreversibility process as shown in Fig. 2. In a previous study, performed using the CASPT2/MM methodology for the $dG_{18}xdC_{18}$ system, i.e., a 18-base-pair-long double helix of poly(C)-poly(G) surrounded by water molecules [45], we determined the barrierless path connecting the CBC S_1 state with the dimer CI, which may later lead to the separation of the monomers. Although the required excitation energy in the dimer to initiate the photoreversion process (4.57–5.64 eV, within the UV-C range) is higher than the energy needed for the monomer excitation, it represents a competitive photoreaction that may reduce the yield of the photoadduct. The formation of CC photodimers was studied by Tommasi et al. [18] under UV-B and UV-C irradiations, showing an increase in the CPD production when UV-B was used, in clear agreement with the results obtained here.

4 Conclusions

The formation of cyclobutane pyrimidine dimers following UV absorption of pairs of stacked DNA/RNA nucleobases has been studied for the homodimers of thymine, uracil, cytosine, and 5-methylcytosine at the theoretical, ab initio CASPT2 multiconfigurational level. Determination of states minima, minimum reaction paths, and conical intersections in the low-lying singlet states of the dimers and monomers has led us to establish a unified mechanism for the adduct formation, which proceeds via a nonadiabatic [2 + 2] photocycloaddition reaction in the singlet manifold. A sheared-like conical intersection connecting the S_1 and S_0 states of the dimer, CI_{dim} $(S_0/S_1)_{CI}$, is the funnel controlling the reactive process. The relative position of the dimer CI with respect to stable excimer structures or the monomer decay CI region determines the efficiency of the photoreactivity. Thus, the dimer CI is the lowest-energy structure in thymine and uracil homodimers, lacking other direct competitive decay processes and favoring the higher efficiency observed in the formation of the CBT and CBU adducts. In contrast, the dimer CI computed in cytosine and 5-methylcytosine is close in energy to the most stable excimer conformation, displaying a face-to-face quasi-parallel structure, and also to the corresponding monomer CIs. Those features can easily compete with the nonadiabatic dimerization reaction decreasing its rates and yields. In fact, the stable excimer structure is lower in energy than the dimer CI in the latter systems, in which a 0.2- and 0.1-eV barrier, respectively, is found to reach the degeneracy region. Those profiles can explain the higher yields found in TT sites when compared with CC. Also, it is shown that methylation, in T and m^5C with respect to U and C, respectively, destabilizes the excimer structures with respect to the CI. Thus, in the case of cytosine, the methylation favors the probability for dimerization by decreasing energy barriers leading to the reaction. It must be highlighted that a high level of theory is required to obtain accurate profiles. CASPT2, including exhaustively the correlation energy, in contrast to simply CASSCF (or lower level approaches like TDDFT) is required to remove undesired differential correlation effects [33, 46], whereas the inclusion of the BSSE effect is essential to obtain accurate and comparable binding energies among the different systems.

Acknowledgments In memory of Luis Serrano-Andrés, he was an excellent scientist and friend. Research supported by projects CTQ2007-61260, CTQ2010-14892, and CSD2007-0010 Consolider-Ingenio in Molecular Nanoscience of the Spanish MEC/FEDER and the Generalitat Valenciana. It has also received funding from the European Research Council under the European Community's Seventh Framework Programme (FP7/2007-2013)/ERC grant agreements n° 255363 and n° 251955.

References

1. Olivera BM (1978) Proc Natl Acad Sci USA 75:238–242
2. Setlow RB (1974) Proc Natl Acad Sci USA 71:3363–3366
3. Cadet J, Vigny P (1990) In: Morrison H (ed) Bioorganic photochemistry. Wiley, New York, p 1
4. Friedberg EC, Walker GC, Siede W, Wood RD, Schultz RA (2006) Ellenberger T (ed) DNA Repair and mutagenesis. ASM Press, Washington, DC
5. Björn LO, McKenzie RL (2008) In: Björn LO (ed) Photobiology. The science of life and light. Springer, New York, p 503
6. Douki T, Cadet J (2001) Biochemistry 40:2495–2501
7. Schuch AP, Menck CFM (2010) J Photochem Photobiol B Biol 99:111–116
8. You YH, Li C, Pfeifer GP (1999) J Mol Biol 293:493–503
9. You YH, Pfeifer GP (2001) J Mol Biol 305:389–399
10. Ikehata H, Masuda T, Sakata H, Ono T (2003) Environ Mol Mutagen 41:280–292
11. Lee DH, Pfeifer GP (2003) J Biol Chem 278:10314–10321
12. Shetlar MD, Basus VJ, Falick AM, Mujeeb A (2004) Photochem Photobiol Sci 3:968–979
13. Friso S, Choi SW, Dolnikowski GG, Selhub J (2002) Anal Chem 74:4526–4531
14. Adams RLP, Burdon RH (1984) Molecular biology of DNA methylation. Springer, New York, pp 6–7 (Table 1.2)
15. Ehrlich M, Dove MF (1983) Photobiochem Photobiophys 6:121–126
16. Ehrlich M, Dove MF, Huang LH (1986) Photobiochem Photobiophys 11:73–79
17. Mitchell DL (2000) Photochem Photobiol 71:162–165
18. Tommasi S, Denissenko MF, Pfeifer GP (1997) Cancer Res 57:4727–4730
19. Schreier WJ, Schrader TE, Soller FO, Gilch P, Crespo-Hernández CE, Swaminathan VN, Carell T, Zinth W, Kohler B (2007) Science 315:625–629
20. Roca-Sanjuán D, Olaso-González G, González-Ramírez I, Serrano-Andrés L, Merchán M (2008) J Am Chem Soc 130:10768–10779
21. Boggio-Pasqua M, Groenhof G, Schäfer LV, Grubmüller H, Robb MA (2007) J Am Chem Soc 129:10996–10997

22. Blancafort L, Migani A (2007) J Am Chem Soc 129:14540–14541
23. Serrano-Pérez JJ, González-Ramírez I, Coto PB, Merchán M, Serrano-Andrés L (2008) J Phys Chem B 112:14096–14098
24. Zhang WY, Yuan SA, Li AY, Dou YS, Zhao JS, Fang WH (2010) J Phys Chem C 114:5594–5601
25. González-Ramírez I, Climent T, Serrano-Pérez JJ, González-Luque R, Merchán M, Serrano-Andrés L (2009) Pure Appl Chem 81:1695–1705
26. Climent T, González-Ramírez I, González-Luque R, Merchán M, Serrano-Andrés L (2010) J Phys Chem Lett 1:2072–2076
27. González-Luque R, Climent T, González-Ramírez I, Merchán M, Serrano-Andrés L (2010) J Chem Theor Comp 6:2103–2114
28. Bosca F, Lhiaubet-Vallet V, Cuquerella MC, Castell JV, Miranda MA (2006) J Am Chem Soc 128:6318–6319
29. Kwok WM, Ma C, Phillips DL (2008) J Am Chem Soc 130:5131–5139
30. Xiaoyi L, Eriksson LA (2005) Chem Phys Lett 401:99–103
31. Andersson K, Malmqvist PÅ, Roos BO (1992) J Chem Phys 96:1218–1226
32. Roos BO, Andersson K, Fülscher MP, Malmqvist PÅ, Serrano-Andrés L, Pierloot K, Merchán M (1996) Adv Chem Phys 93:219
33. Merchán M, Serrano-Andrés L (2005) In: Olivucci M (ed) Computational photochemistry. Elsevier, Amsterdam, p 35
34. Serrano-Andrés L, Merchán M (2009) J Photochem Photobiol C Photochem Rev 10:21–32
35. Serrano-Andrés L, Merchán M, Lindh R (2005) J Chem Phys 122:104107–104110
36. Boys SF, Bernardi F (2002) Mol Phys 100:65
37. Olaso-González G, Merchán M, Serrano-Andrés L (2009) J Am Chem Soc 131:4368–4377
38. Aquilante F, De Vico L, Ferré N, Ghigo G, Malmqvist PÅ, Pedersen T, Pitonak M, Reiher M, Roos BO, Serrano-Andrés L, Urban M, Veryazov V, Lindh R (2010) J Comp Chem 31:224–247
39. Forsberg N, Malmqvist PÅ (1997) Chem Phys Lett 274:196–204
40. Crespo-Hernández CE, De La Harpe K, Kohler B (2008) J Am Chem Soc 130:10844–10845
41. Takaya T, Su C, De La Harpe K, Crespo-Hernández CE, Kohler B (2008) Proc Natl Acad Sci USA 105:10285–10290
42. Crespo-Hernández CE, Cohen B, Hare PM, Kohler B (2004) Chem Rev 104:1977–2020
43. Serrano-Andrés L, Merchán M (2008) Shukla MK, Leszczynski J (eds) Photostability and photoreactivity in biomolecules: quantum chemistry of nucleic acid base monomers and dimers. In: Radiation induced molecular phenomena in nucleic acids: a comprehensive theoretical and experimental analysis. Springer, The Netherlands, p 435
44. Douki T, Cadet J (2001) Biochemistry 40:2495–2501
45. Roca-Sanjuán D, Olaso-González G, Rubio M, Coto PB, Merchán M, Ferré N, Ludwig V, Serrano-Andrés L (2009) Pure Appl Chem 81:743–754
46. Serrano-Andrés L, Merchán M (2005) J Mol Struct Theochem 729:99–108